Improving sensitivity of existing surface plasmon resonance systems with grating-coupled short-range surface plasmons

Elham Babaei, Zohreh Sharifi, and Reuven Gordon

2019

The final publication is available at:

https://doi.org/10.1364/JOSAB.36.00F144

Citation for this paper:

Babaei, E., Sharifi, Z., & Gordon, R. (2019). Improving sensitivity of existing surface plasmon resonance systems with grating-coupled short-range surface plasmons. Journal of the Optical Society of America B, 36(8), F144–F148. https://doi.org/10.1364/JOSAB.36.00F144

Improving Sensitivity of Existing Surface Plasmon Resonance Systems with Grating Coupled Short Range Surface Plasmons

ELHAM BABAEI[1], ZOHREH SHARIFI[1], AND REUVEN GORDON[1,*]

[1] Department of Electrical and Computer Engineering, University of Victoria, Victoria, BC, v8P5C2
[*] Corresponding author: rgordon@uvic.ca

Compiled April 20, 2023

Here we show that surface plasmon resonance sensors that typically use 760 nm wavelength Kretschmann-Raether coupling to a 50 nm thick gold film can have 3 times higher surface sensitivity by using local resonances from periodically arranged short-range modes in the same configuration. Considering shot noise, the resolution was found to improve four-fold. This was calculated by matching the design wavelength and minimum angle as calculated by rigorous coupled wave analysis, giving a period of 250 nm in a 10 nm thick gold film and a gap length of 40 nm. Finite difference time domain simulations were used to confirm that the short-range modes correspond to a localized surface plasmon resonances. The present short-range plasmon approach can be used to improve the sensitivity in monitoring biomolecule interactions.

http://dx.doi.org/10.1364/ao.XX.XXXXXX

1. INTRODUCTION

Conducting surfaces permit guided waves called surface plasmon polaritons (SPPs), the mathematical solutions of which have been known for over a century [1]. A prism can be used to couple light into these surface waves, matching the wave-vector in the high-index prism to the wave-vector of the surface plasmon [2, 3]. Since the metal is lossy, light is absorbed at the coupling condition and this leads to a dip in the reflection [3].

The SPP is exponentially bound to the surface, which gives good sensitivity to changes in refractive index near the surface. This is the premise behind the commercialized surface plasmon resonance (SPR) biosensors [4]. These commercial systems have been engineered with consideration of many factors: the light source wavelength, the light source type (LED vs. laser), the metal type, the metal thickness, the detector type (single channel vs. detector array), the data acquisition (dynamic range, analogue to digital conversion and acquisition time) and cost. With all of this engineering already in place and many such machines in laboratories around the world, it is interesting to consider leveraging the existing commercial SPR platform while using a more sensitive sensor chip.

One potential direction to obtain even greater surface sensitivity is to use short-range surface plasmon (SRSP) modes [5, 6]. In particular, insulator-metal-insualtor (IMI) structures permit SRSP modes that become more tightly confined to the surface as the thickness of the metal is reduced. This leads to greater surface sensitivity. Here we consider the use of these SRSP modes in sensing applications while retaining the popular prism coupling configuration.

The SRSP modes have a larger propagation constant than the usual SPPs. Therefore, to couple into these modes while retaining the same Kretschmann geometry as the usual 50 nm thick gold film, we employ a periodic structure with localized surface plasmon (LSP) resonances. There is a clear connection between the SRSP modes and the LSP resonances of a metal stripe: the LSP resonances arise from the propagation and reflection of the SRSP modes [7]. We note also that the terminology of short-range surface plasmon polariton, SR-SPP, is also used to emphasize that the SRSP is a polariton (consisting of a hybridization between field and charge polarization). Another feature of these modes is that they are more lossy; therefore, it is expected that their reflection dip will broaden upon coupling.

In this paper, we find a design for SRSP sensing using a rectangular stripe grating and a 10 nm thick gold film. The 10 nm gold is thick enough to allow for continuous films with standard deposition techniques. Using rigorous coupled wave analysis (RCWA), we

find that the surface sensitivity of these films to an adlayer is 3.3 times higher in terms of angle units and the resolution is improved by four-fold, while operating in the same range as commercial SPR systems. Therefore, we believe these chips may be used for more sensitive SPR sensing in the near future.

2. DESIGN

A. Standard SPR Sensing

Figure 1 shows the schematics of a typical surface coupling for conventional SPR and the proposed IMI-grating structure. A metal film is confined between two dielectric layers. Incident light couples to the SPP in the case of SPR. SPR occurs when the incident angle is greater than the critical angle. The parallel component of incident light should match the surface plasmon wave-vector. The minimum of reflection occurs when the energy of the incident photon is transferred to surface plasmon wave.

Figure 1 (a) shows the standard configuration for a uniform 50 nm gold film. Uniform films are suitable for SPPs of a single surface. Figure 1 (b) shows the proposed scheme with a periodic gold structure on glass. This structure allows decreasing gold thickness to 10 nm, which increases the confinement of the field significantly.

For conventional SPP coupling, the light is angled in the prism to match the SPP wave-vector. The SPP wave-vector is given by:

$$k_{\mathrm{SP}} = k_0 \sqrt{\frac{\epsilon_m \epsilon_d}{\epsilon_m + \epsilon_d}} \tag{1}$$

where $k_0 = 2\pi/\lambda$ ($\lambda = 760$ nm, the wavelength of commercial systems, e.g., from Biacore [8]), ϵ_m is the relative permittivity of the metal, ϵ_d is the relative permittivity of the adjacent dielectric (in this case water). The wave-vector in the prism is given by:

$$k_{\mathrm{prism}} = k_0 n_{\mathrm{prism}} \sin\theta \tag{2}$$

where θ is the angle of incidence in the prism and n_{prism} is the prism's refractive index. In this case the SPP coupling occurs where $k_{\mathrm{SP}} = k_{\mathrm{prism}}$, as shown in Figure 2.

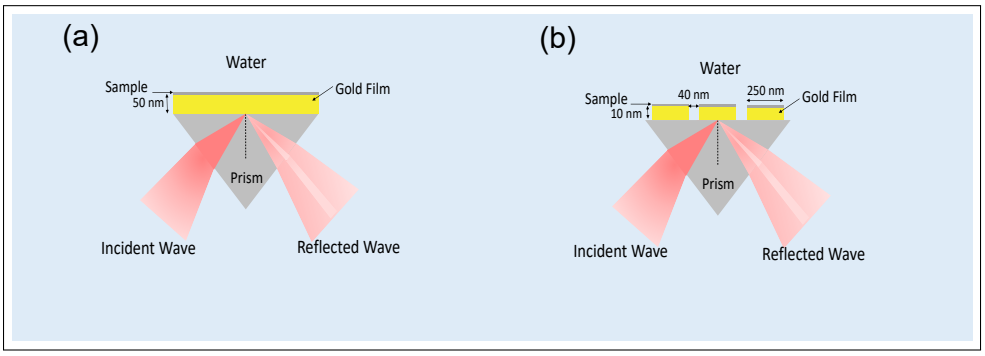

Fig. 1. (a) Prism coupled SPR structure for a 50 nm gold film. (b) Modified structure for a 10 nm gold film using a grating.

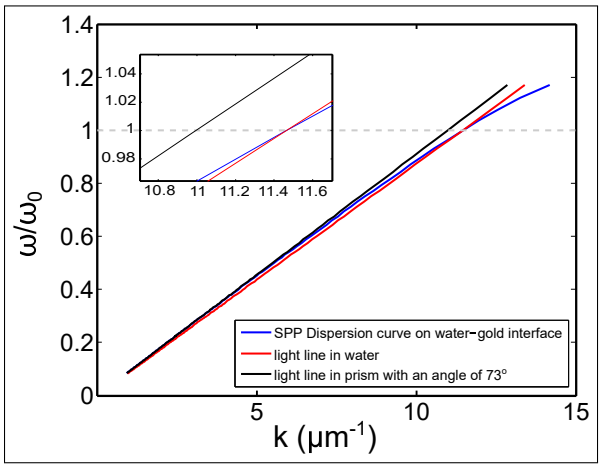

Fig. 2. Dispersion for coupling to surface plasmon at water-gold interface when incident from glass-gold side of the prism. The intersection point is at 73°, which gives a dip due to losses in the SPP.

Figure 3 shows the reflection of a 50 nm gold film when incident through a prism as a function of incident angle. The refractive index of the prism is 1.5 and the top layer is considered to be water with refractive index 1.33. It is clear from this figure that the

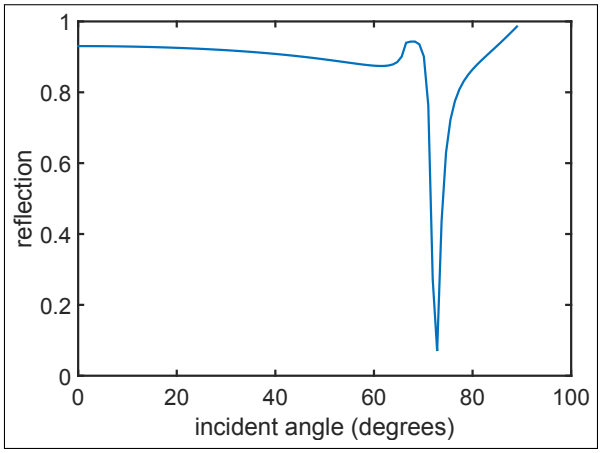

Fig. 3. Reflection from a 50 nm thick gold film on glass with a water top layer for different incident angles.

reflection dip of optimal SPP coupling occurs at around 73°, as expected from the coupling analysis above. (Of course, RCWA is not required for this analysis since standard transfer matrix theory is applicable to a uniform layer). It is noted that the surface plasmon dispersion is for a semi-infinite surface, and so the treatment of using wave coupling through the film is approximate, whereas the RCWA is not [9].

B. SRSP Grating-Assisted Coupling

The propagation constant of a surface plasmon wave on a thin metal film with thickness of h which is bounded by two dielectric media, with subscripts 1 and 3, is determined by following equations [10]:

$$\tanh p_m h(1 + s_1 s_3) = -(s_1 + s_3) \tag{3}$$

$$s_1 = \frac{p_1}{p_m}\frac{\epsilon_m}{\epsilon_1} \tag{4}$$

$$s_3 = \frac{p_3}{p_m}\frac{\epsilon_m}{\epsilon_3} \tag{5}$$

$$p_1^2 = \beta^2 - k_0^2\epsilon_1 \tag{6}$$

$$p_m^2 = \beta^2 - k_0^2\epsilon_m \tag{7}$$

$$p_3^2 = \beta^2 - k_0^2\epsilon_3 \tag{8}$$

where β is the wavevector of the SRSP and k_0 is the free-space wavevector.

Using these equations, we find that the effective index of the SRSP is 2.58. From this, one can couple to the SRSP by using a periodic structure period of 636 nm to match the wavevector of light in the prism to that of the SRSP using the equation:

$$k_{\text{prism}} + K_G = \beta \tag{9}$$

where:

$$K_G = \frac{2\pi}{\Lambda} \tag{10}$$

with Λ being the grating period and β is the propagation constant of the SRSP.

We attempted this configuration and found that coupling was weak (a dip in the reflection of only around 30 %). As a result, we considered the possibility of using stronger resonances found in LSPs in the array format.

C. LSP Coupling

LSPs are supported by finite metal nanostructures. We first employed RCWA to study periodic LSP structures for prism coupling. RCWA is typically used to study the interaction of an electromagnetic wave with a surface plasmons on a metallic relief grating. RCWA is also a reliable approach to determine dips in reflection as a function of wavelength and angle [11, 12].

Figure 4 shows reflection spectrum for different structures using RCWA method. p is the period of the grating and g is the size of the gap. As shown in the figure for grating period of 250 nm and gap length of 40 nm, the dip occurred for 760 nm incident light, which is the desired operating wavelength and angle of incidence.

To verify that the origin of this dip is from the LSP resonance, we performed finite-difference time-domain (FDTD) simulations of an isolated structure using the commercial package by Lumerical. We use a grid size of 0.2 nm in the direction perpendicular to the layers and 1 nm in the direction of SRSP propagation. The total domain simulated was 280 nm by 5.75 μm, and bounded by perfectly matched layers. The gold layer was taken from the Palik database. The gold thickness was 10 nm, and its length was 210 nm. A dipole

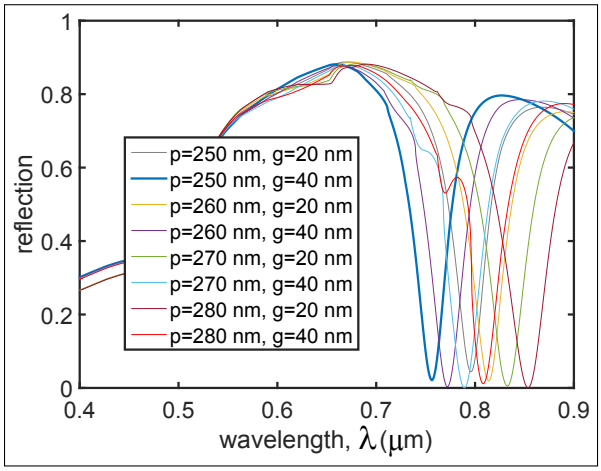

Fig. 4. Reflection spectra periodic structure supporting SRSP mode with an incidence angle of 73°. The period, p, and gap g were varied in each curve to find the case which is most closely matched to the operating wavelength of 760 nm.

source was placed at one end of the rectangular gold structure and the field intensity was monitored at the peak at the other end of the structure.

Figure 5 shows the electric field intensity at the end of the gold nanostructure, with a clear peak at the desired operation wavelength of 760 nm. Figure 6 shows the field intensity at the opposite end of the rectangular structure, with clear edge enhancement, but also strongly confined light at the metal surface. To support the connection between the LSP resonance and SRSP mode, we plot the longitudinal electric field from the FDTD simulation and compare it with the longitudinal electric field of the SRSP mode (calculated using the finite difference technique), as shown in Figure 7. Good agreement is seen in the field amplitude profile, with some discrepancy at the edges due to the different boundary conditions.

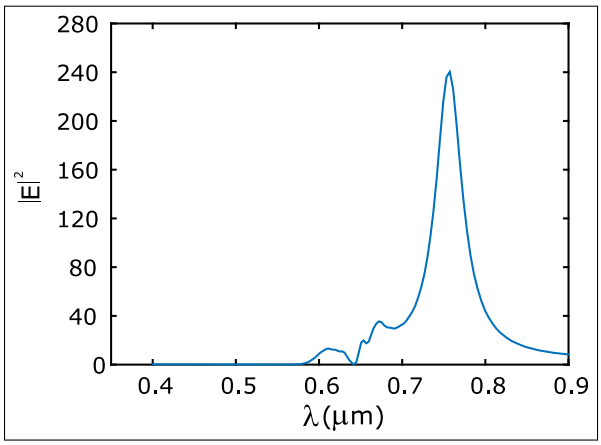

Fig. 5. Electric field intensity monitored near a 10 nm thick and 210 nm long rectangular gold structure on glass with a water surrounding. The peak in the LSP resonance is at 760 nm as desired for the SPR sensor configuration.

3. SENSING PERFORMANCE

A. Sensitivity Calculations

To investigate the improved sensitivity of the resonant periodic structure supporting the SRSP, a 1 nm adlayer is applied on the top of the gold with refractive index 1.5. Figure 8 shows the reflection for different angles of incidence, both for a 50 nm thick gold film and for the 10 nm thick periodic structure. In each figure, the reflection is plotted for the bare structure and the structure with an adlayer. As demonstrated in the inset figures, the 10 nm gold periodic structure has 3.3 times higher sensitivity than for 50 nm continuous gold. (Note, that restricting the adlayer to the top surface is done for analytic simplicity, and may be achieved in practice by masking the side-walls).

The figure of merit commonly used is the ratio between the shift and the width of the dip (both in degrees). For the example provided, the figure of merit obtained was 0.05 and 0.14 for 10 nm and 50 nm gold structures on glass at the 20% reflection level. The noise properties, however, define the resolution of the sensor and ultimately limit define performance [8].

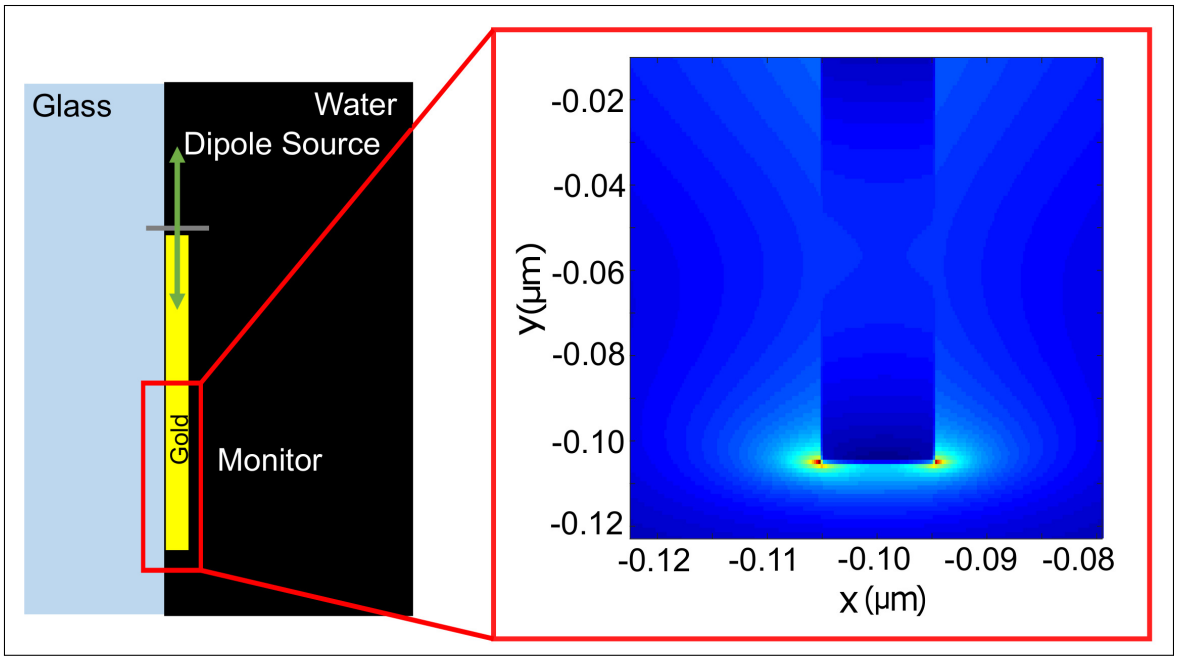

Fig. 6. The field intensity distribution at the LSP resonance.

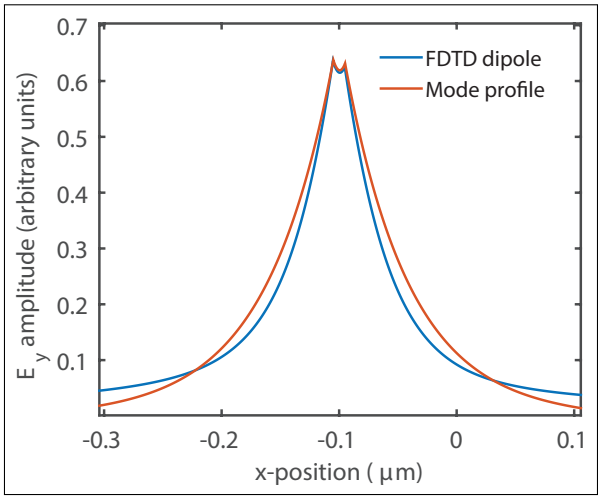

Fig. 7. Longitudinal electric field amplitude at $y = -53$ nm for FDTD simulation (as shown in Figure 6). For comparison, the longitudinal field distribution of the SRSP mode profile is also given.

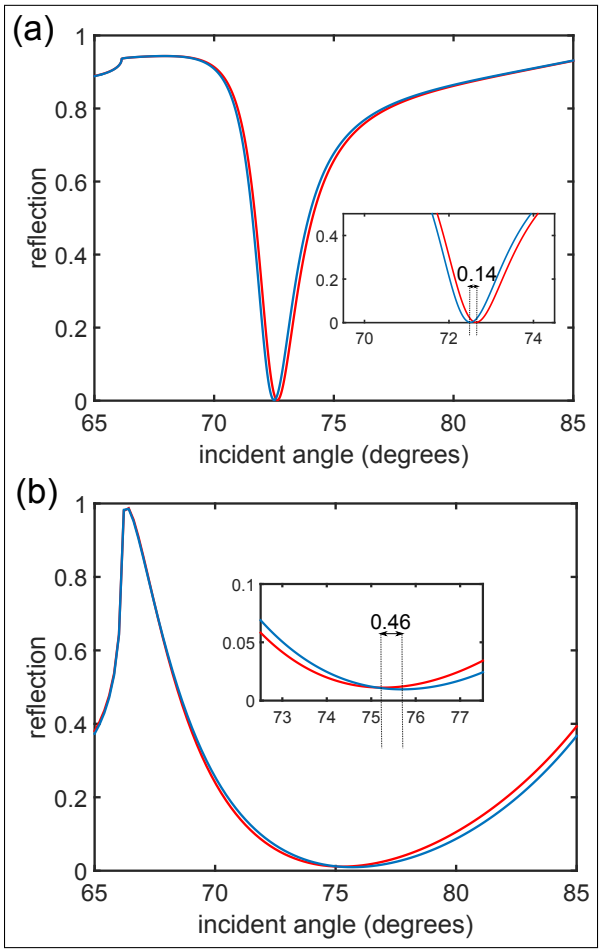

Fig. 8. Sensitivity calculations for (a) a 50 nm thick gold film with and without a 1 nm adlayer, and (b) a 10 nm thick gold film with 250 nm period and 210 nm length of each gold segment, with and without a 1 nm adlayer. The insets are shown to clearly depict the angle shifts with the adlayer in each case.

B. Resolution Calculations

To compare the resolution of the SPR sensing for a gold film with the thickness of 50 nm and the structured film with 10 nm thickness, we added shot noise to the digitized reflection. The digitization used 1024 bins for angle of incidence and 4096 bins for reflection intensity. We fit the noisy response to various adlayer index values (thickness 1 nm), and repeated the procedure to ensure a suitably averaged response. In this way, the resolution was determined to be 8×10^{-5} RIU/nm for 50 nm gold and 2×10^{-5} RIU/nm for 10 nm gold SRSP structure.

4. DISCUSSION

It is clear from the analysis presented that the 10 nm thick gold film with a stripe grating structure has 3.3 times higher sensitivity and 4 times improved resolution. Many have suggested that having a narrower peak will improve the performance of SPR detection systems because it allows for more precisely determining the position of the reflection dip. As noted above, for this reason a figure-of-merit of wavelength shift divided by peak width is often used [13]. There are arguments to suggest that this is not always true. Consider the extreme case where the peak is much narrower than even one pixel spacing of the detector array, then there is no change in the signal detected for a sub-pixel sized shift with an adlayer. Therefore, having a very narrow peak can give no signal at all, even though the usual figure-of-merit is huge.

Here, we have done the resolution calculations and found that the broader peak actually allows for improved resolution because the signal is supported by a greater number of bins (therefore, the noise in each bin can be averaged to reduce the overall noise). This noise analysis focuses on shot noise, where the noise is proportional to the square root of the detected counts. A well-engineered system will be shot noise limited [8].

Low cost fabrication of these grating structures is also an important consideration. We believe that these structures can be readily manufactured at low cost using existing template stripping approaches [14].

It is possible to push the sensitivity even higher by looking at ultra-thin gold films. While 10 nm continuous gold films are commercially available, special methods can be used to create continuous films down to 5.4 nm that are stable under ambient conditions [15].

We are aware of extremely high sensitivity demonstrations using nanorods (and similar works) [16]. While it is interesting to consider such approaches further, there are potential advantages of our design. We have already mentioned that our design is compatible with existing SPR instruments, and may be readily mass produced using template stripping or other similar approaches. In addition, our design uses a mainly flat surface and so fouling that can occur with highly structured surfaces is not as big a concern.

5. CONCLUSIONS

In this work, we consider a periodic SRSP sensor design that is compatible with existing commercial SPR sensors. The SRSP works by coupling to the LSP resonance of a rectangular structure. The design shows a 3.3 times higher surface sensitivity, which is promising for high-performance detection applications (such as low index contrast materials or sub-monolayer absorption). A noise analysis shows that the resolution also improves four-fold in the SRSP design.

6. FUNDING INFORMATION

This work is supported by an NSERC Discovery Grant.

REFERENCES

1. J. Zenneck, “Über die fortpflanzung ebener elektromagnetischer wellen längs einer ebenen leiterfläche und ihre beziehung zur drahtlosen telegraphie,” Annalen der Physik **328**, 846–866 (1907).
2. E. Kretschmann and H. Raether, “Radiative decay of non radiative surface plasmons excited by light,” Zeitschrift für Naturforschung A **23**, 2135–2136 (1968).
3. E. Kretschmann, “Die bestimmung optischer konstanten von metallen durch anregung von oberflächenplasmaschwingungen,” Zeitschrift für Physik A Hadron. nuclei **241**, 313–324 (1971).
4. B. Liedberg, C. Nylander, and I. Lundström, “Biosensing with surface plasmon resonance—how it all started,” Biosens. Bioelectron. **10**, i–ix (1995).
5. E. Economou, “Surface plasmons in thin films,” Phys. Rev. **182**, 539 (1969).
6. P. Berini, “Bulk and surface sensitivities of surface plasmon waveguides,” New J. Phys. **10**, 105010 (2008).
7. G. Della Valle, T. Søndergaard, and S. I. Bozhevolnyi, “Plasmon-polariton nano-strip resonators: from visible to infra-red,” Opt. Express **16**, 6867–6876 (2008).
8. M. Piliarik and J. Homola, “Surface plasmon resonance (spr) sensors: approaching their limits?” Opt. express **17**, 16505–16517 (2009).
9. G. Rosenblatt, B. Simkhovich, and M. Orenstein, “Brewster plasmons: new optical degrees of freedom driving the forced repose of nanostructures (conference presentation),” in *Metamaterials, Metadevices, and Metasystems 2018,* , vol. 10719 (International Society for Optics and Photonics, 2018), p. 107191R.
10. C. Yeh and F. I. Shimabukuro, *The essence of dielectric waveguides* (Springer, 2008).
11. M. Moharam and T. K. Gaylord, “Rigorous coupled-wave analysis of metallic surface-relief gratings,” JOSA a **3**, 1780–1787 (1986).
12. S. Park, G. Lee, S. H. Song, C. H. Oh, and P. S. Kim, “Resonant coupling of surface plasmons to radiation modes by use of dielectric gratings,” Opt. Lett. **28**, 1870–1872 (2003).
13. P. Offermans, M. C. Schaafsma, S. R. Rodriguez, Y. Zhang, M. Crego-Calama, S. H. Brongersma, and J. Gómez Rivas, “Universal scaling of the figure of merit of plasmonic sensors,” ACS Nano **5**, 5151–5157 (2011).
14. P. Nagpal, N. C. Lindquist, S.-H. Oh, and D. J. Norris, “Ultrasmooth patterned metals for plasmonics and metamaterials,” Science **325**, 594–597 (2009).

15. A. Kossoy, V. Merk, D. Simakov, K. Leosson, S. Kéna-Cohen, and S. A. Maier, "Optical and structural properties of ultra-thin gold films," Adv. Opt. Mater. **3**, 71–77 (2015).
16. A. Kabashin, P. Evans, S. Pastkovsky, W. Hendren, G. Wurtz, R. Atkinson, R. Pollard, V. Podolskiy, and A. Zayats, "Plasmonic nanorod metamaterials for biosensing," Nat. Mater. **8**, 867 (2009).